POLITECNICO DI TORINO
Repository ISTITUZIONALE

Prismatic Delta Robot: A Lagrangian Approach

Original
Prismatic Delta Robot: A Lagrangian Approach / Colombo, F.; Lentini, L.. - 84:(2020), pp. 315-324. [10.1007/978-3-030-48989-2_34]

Availability:
This version is available at: 11583/2839078 since: 2020-07-09T08:36:05Z

Publisher:
Springer

Published
DOI:10.1007/978-3-030-48989-2_34

Terms of use:

This article is made available under terms and conditions as specified in the corresponding bibliographic description in the repository

Publisher copyright
Springer postprint/Author's Accepted Manuscript

This version of the article has been accepted for publication, after peer review (when applicable) and is subject to Springer Nature's AM terms of use, but is not the Version of Record and does not reflect post-acceptance improvements, or any corrections. The Version of Record is available online at: http://dx.doi.org/10.1007/978-3-030-48989-2_34

(Article begins on next page)

19 April 2024

Prismatic Delta Robot: a Lagrangian Approach

Colombo Federico[0000-0002-1054-236X] and Lentini Luigi[0000-0003-3770-3773]

Department of Mechanical and Aerospace Engineering, Politecnico di Torino, Torino, Italy

federico.colombo@polito.it
luigi.lentini@polito.it

Abstract. This paper shows the kinematic and dynamic model of a prismatic Delta robot designed for a 3D printer. After description of the direct and inverse kinematic algorithms, the forces on the actuated prismatic joints are computed with the lagrangian approach.
Examples of actuators forces computed with the lagrangian approach are shown in case of Lissajous type path imposed on the end effector (inverse kinematics) and traveled at constant speed. The results are checked with the energy conservation principle. The effect of inertia forces is evaluated at different printing speeds.

Keywords: Prismatic Delta robot, Lagrangian approach, parallel robots, dynamic modelling.

1 Introduction

Delta robot structure is employed is several industrial applications, such as pick and place machines and 3D printers. An evident advantage respect to other structures, such as the cartesian one, is the higher acceleration that can be reached, due to the small moving masses.

This robot was invented in 80s by Clavel [1]. It was then introduced into the market, initially for pick and place operation and packaging, then also for haptic controllers and other purposes (e.g. medical and pharmaceutical), last but not least for 3D printing [2,3].

The kinematics of the delta robot with rotating actuators is proposed in [4], while in [5] the kinematic analysis is performed for the delta robot with prismatic actuators, with particular attention to singularities. The kinematic study for this structure is also carried out in [6].

About the dynamics, there are three methods to determine the actuators forces in dynamic conditions [7]: the Newton-Euler procedure, the principle of virtual works and the Lagrange's equation with multipliers formalism. The principle of virtual work has been applied in [8] to calculate the dynamics of the prismatic delta robot. The lagrangian approach was employed to study the dynamics of a delta robot with rotational actuators [9], but to the best of author's knowledge, this approach has not yet been

employed to the delta robot with prismatic actuators. This paper is aimed at covering this literature lack.

2 The prismatic Delta robot

The architecture of the delta robot with prismatic joints is depicted in Fig.1. The robot is a parallel machine composed by a platform and three legs each of them is a serial kinematic chain of type $P(SS)_2$. Due to the presence of the parallelograms in each leg, the platform can only translate along the three directions. The prismatic actuated joints are vertical and connect the three carts to the fixed basement. Points A_1, A_2 and A_3 are defined in the middle of the short sides of the parallelograms in correspondence of the carts, while points P_1, P_2 and P_3 are defined in the middle of the opposite sides, in correspondence of the platform. Points B_1, B_2 and B_3 are the vertical projections of points A_1, A_2 and A_3 on the basement plane. A fixed reference system OXYZ is located in the center of the basement, with X axis parallel to segment B_1B_2 and oriented from B_1 to B_2 and Y axis oriented towards point B_3. Both triplets $B_1B_2B_3$ and $P_1P_2P_3$ identify equilateral triangles attached to the basement and to the platform respectively. The side lengths of these triangles are indicated as s_B (triangle on basement) and s_P (triangle on platform). Point P is located in the center of the platform.

The dofs associated to the prismatic joints are indicated with q_1, q_2 and q_3 and represent the coordinates along Z axis of points A_1, A_2 and A_3 respect to fixed reference frame.

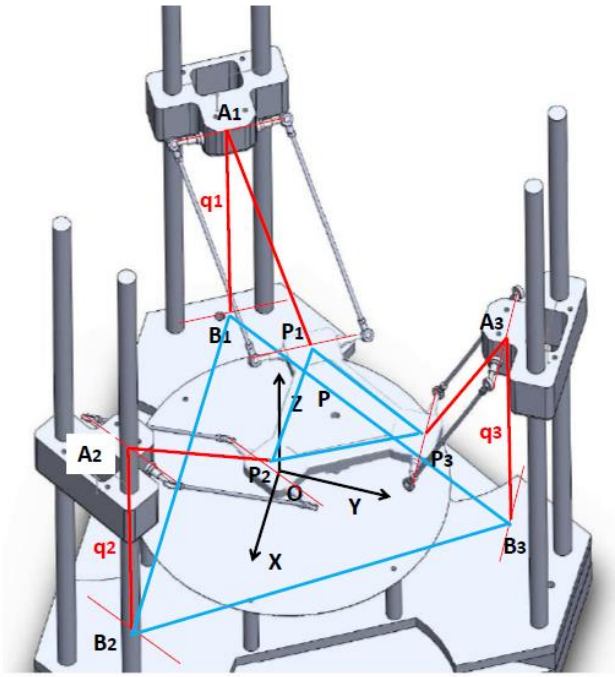

Fig. 1. Architecture of the prismatic Delta robot

3 Kinematics

The direct kinematics study involves the calculation of position, velocity and acceleration of the platform when the input trajectories in prismatic joints are known. Vice versa, the inverse kinematics involves the calculation of the joints trajectories when the motion of the platform is supposed to be known.

The closure equations are the following:

$$\begin{aligned} \boldsymbol{OB}_1 + \boldsymbol{B}_1\boldsymbol{A}_1 + \boldsymbol{A}_1\boldsymbol{P}_1 + \boldsymbol{P}_1\boldsymbol{P} = \boldsymbol{OP} \\ \boldsymbol{OB}_2 + \boldsymbol{B}_2\boldsymbol{A}_2 + \boldsymbol{A}_2\boldsymbol{P}_2 + \boldsymbol{P}_2\boldsymbol{P} = \boldsymbol{OP} \\ \boldsymbol{OB}_3 + \boldsymbol{B}_3\boldsymbol{A}_3 + \boldsymbol{A}_3\boldsymbol{P}_3 + \boldsymbol{P}_3\boldsymbol{P} = \boldsymbol{OP} \end{aligned} \tag{1}$$

Imposing that the length of segments $\boldsymbol{A}_1\boldsymbol{P}_1$, $\boldsymbol{A}_2\boldsymbol{P}_2$ and $\boldsymbol{A}_3\boldsymbol{P}_3$ is constant in time and equal to *l*, the length of the long side of the parallelograms, the following non-linear equations are derived:

$$\begin{aligned} \left(x_P + \frac{S_B}{2} - \frac{S_P}{2}\right)^2 + \left(y_P + \frac{S_B}{2\sqrt{3}} - \frac{S_P}{2\sqrt{3}}\right)^2 + (z_P - q_1)^2 = l^2 \\ \left(x_P - \frac{S_B}{2} + \frac{S_P}{2}\right)^2 + \left(y_P + \frac{S_B}{2\sqrt{3}} - \frac{S_P}{2\sqrt{3}}\right)^2 + (z_P - q_2)^2 = l^2 \\ {x_P}^2 + \left(y_P - \frac{S_B}{\sqrt{3}} + \frac{S_P}{\sqrt{3}}\right)^2 + (z_P - q_3)^2 = l^2 \end{aligned} \tag{2}$$

3.1 Direct kinematics

Known q_1, q_2 and q_3 and their first and second time derivatives, the direct kinematics allows to compute the coordinates x_P, y_P and z_P of point P and their time derivatives. As system (2) is non-linear, it can be solved with an iterative method such as Newton Raphson or the three spheres intersection algorithm [6].

The velocities are easily computed solving a linear system resulting from the differentiation of system (2). These equations can be written in a more compact way using the matrix notation:

$$J_x \begin{Bmatrix} \dot{x}_P \\ \dot{y}_P \\ \dot{z}_P \end{Bmatrix} = J_q \begin{Bmatrix} \dot{q}_1 \\ \dot{q}_2 \\ \dot{q}_3 \end{Bmatrix} \tag{3}$$

where J_x and J_q are the Jacobian matrixes. It results

$$\begin{Bmatrix} \dot{x}_P \\ \dot{y}_P \\ \dot{z}_P \end{Bmatrix} = J_x^{-1} J_q \begin{Bmatrix} \dot{q}_1 \\ \dot{q}_2 \\ \dot{q}_3 \end{Bmatrix} \tag{4}$$

The accelerations are obtained differentiating once more equations system (4) and expressing in matrix notation. It results

$$\begin{Bmatrix} \ddot{x}_P \\ \ddot{y}_P \\ \ddot{z}_P \end{Bmatrix} = J_x^{-1} \left(J_q \begin{Bmatrix} \ddot{q}_1 \\ \ddot{q}_2 \\ \ddot{q}_3 \end{Bmatrix} - \begin{Bmatrix} \dot{x}_P^2 + \dot{y}_P^2 + (\dot{z}_P - \dot{q}_1)^2 \\ \dot{x}_P^2 + \dot{y}_P^2 + (\dot{z}_P - \dot{q}_2)^2 \\ \dot{x}_P^2 + \dot{y}_P^2 + (\dot{z}_P - \dot{q}_3)^2 \end{Bmatrix} \right) \tag{5}$$

3.2 Inverse kinematics

The inverse problem is simpler, as the joint parameters q_1, q_2 and q_3 can be expressed in explicit way as a function of the platform coordinates:

$$\begin{aligned} q_1 &= z_P \pm \sqrt{l^2 - \left(x_P + \frac{S_B}{2} - \frac{S_P}{2}\right)^2 - \left(y_P + \frac{S_B}{2\sqrt{3}} - \frac{S_P}{2\sqrt{3}}\right)^2} \\ q_2 &= z_P \pm \sqrt{l^2 - \left(x_P - \frac{S_B}{2} + \frac{S_P}{2}\right)^2 - \left(y_P + \frac{S_B}{2\sqrt{3}} - \frac{S_P}{2\sqrt{3}}\right)^2} \\ q_3 &= z_P \pm \sqrt{l^2 - {x_P}^2 - \left(y_P - \frac{S_B}{\sqrt{3}} + \frac{S_P}{\sqrt{3}}\right)^2} \end{aligned} \tag{6}$$

The velocities are computed solving system

$$\begin{Bmatrix} \dot{q}_1 \\ \dot{q}_2 \\ \dot{q}_3 \end{Bmatrix} = J_q^{-1} J_x \begin{Bmatrix} \dot{x}_P \\ \dot{y}_P \\ \dot{z}_P \end{Bmatrix} \tag{7}$$

while the accelerations from system

$$\begin{Bmatrix} \ddot{q}_1 \\ \ddot{q}_2 \\ \ddot{q}_3 \end{Bmatrix} = J_q^{-1} \left(J_x \begin{Bmatrix} \ddot{x}_P \\ \ddot{y}_P \\ \ddot{z}_P \end{Bmatrix} - \begin{Bmatrix} \dot{x}_P^2 + \dot{y}_P^2 + (\dot{z}_P - \dot{q}_1)^2 \\ \dot{x}_P^2 + \dot{y}_P^2 + (\dot{z}_P - \dot{q}_2)^2 \\ \dot{x}_P^2 + \dot{y}_P^2 + (\dot{z}_P - \dot{q}_3)^2 \end{Bmatrix} \right) \tag{8}$$

4 The Lagrangian approach

The generalized coordinate vector is defined as $q = [q_1, q_2, q_3, x_p, y_p, z_p]$. This vector can be partitioned in the vector of the independent parameters q_1, q_2, q_3 and the vector of the dependent parameters x_p, y_p, z_p: $q = [q_{ind}, q_{dep}]$.
The mass of each cart is m_{cart}, the mass of each element between the spherical joints is m_{link} (note that there are 6 of these elements), while the mass of the platform is m_{plat}. Fig.2 depicts a simplified lumped mass distribution, in which the mass of each link is splitted in equal parts at the two ends of the link. The extruder nozzle Q is located in point Q at distance PQ below point P. In this work all dissipations are neglected.

The forces Q_1, Q_2, Q_3 on the actuators can be computed from the lagrangian equations (9), valid for j=1 to 6:

$$\frac{d}{dt}\left(\frac{\partial L}{\partial \dot{q}_j}\right) - \frac{\partial L}{\partial q_j} = \sum_{i=1}^{3} \lambda_i \frac{\partial \Gamma_i}{\partial q_j} + Q_j \tag{9}$$

where λ_i (i=1 to 3) are the lagrangian multipliers, which can also be computed solving system (9) and Γ_i (i=1 to 3) are the closure equations. Q_j are the generalized external forces, assumed to be null on platform: $Q = [Q_1, Q_2, Q_3, 0, 0, 0]$.

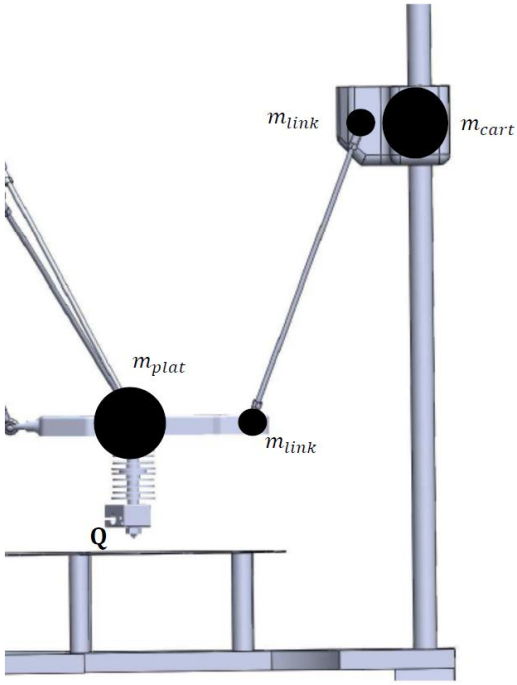

Fig. 2. Simplified lumped mass distribution

System (9) can be written in the following matrix form

$$[A]\{x\} = \{b\} \tag{10}$$

where the unknown parameters vector is

$$\{x\} = \{\lambda_1 \quad \lambda_2 \quad \lambda_3 \quad Q_1 \quad Q_2 \quad Q_3\}^T = \begin{Bmatrix} \{\lambda\} \\ \{Q\} \end{Bmatrix} \tag{11}$$

and the constant vector $\{b\}$ involves both inertia terms and the terms due to gravity:

$$\{b\} = [M]\{\ddot{q}\} + \{F\} \tag{12}$$

Partitioning properly system (10), it is possible to obtain the expressions of the lagrangian multipliers and of the actuators forces:

$$\{\lambda\} = \frac{m_{plat} + 3m_{link}}{2}[J_x^T]^{-1}\{\ddot{q}_{dep}\} + \frac{(m_{plat} + 3m_{link})g}{2}[J_x^T]^{-1}\begin{Bmatrix}0\\0\\1\end{Bmatrix} \tag{13}$$

$$\begin{aligned}\{Q\} = (m_{link} + m_{cart})\left(\begin{Bmatrix}\ddot{q}_1\\\ddot{q}_2\\\ddot{q}_3\end{Bmatrix} + g\begin{Bmatrix}1\\1\\1\end{Bmatrix}\right)\\ + (m_{plat} + 3m_{link})[J_q][J_x^T]^{-1}\left(\begin{Bmatrix}\ddot{x}_p\\\ddot{y}_p\\\ddot{z}_p\end{Bmatrix} + g\begin{Bmatrix}0\\0\\1\end{Bmatrix}\right)\end{aligned} \tag{14}$$

4.1 Static solution

In case the accelerations are null the static solution is obtained:

$$\{Q\} = (m_{link} + m_{cart})g\begin{Bmatrix}1\\1\\1\end{Bmatrix} + (m_{plat} + 3m_{link})[J_q][J_x^T]^{-1}\, g\begin{Bmatrix}0\\0\\1\end{Bmatrix} \tag{15}$$

In the central position (x_P=y_P=0) it results

$$\{Q\} = g\begin{Bmatrix}1\\1\\1\end{Bmatrix}\left(2m_{link} + m_{cart} + \frac{m_{plat}}{3}\right) \tag{16}$$

In a not-centered position the actuators forces are different, but their sum results to be

$$\begin{aligned}Q_1 + Q_2 + Q_3 &= 3(m_{link} + m_{cart})g + (m_{plat} + 3m_{link})g\\ &= (6m_{link} + m_{plat} + 3m_{cart})g\end{aligned} \tag{17}$$

which corresponds to the total gravity force of the suspended masses.

5 Results and discussion

An example of calculation of actuators forces resulting from given trajectories imposed on the platform is shown in this section. The following masses are considered: m_{link}=0.02 kg, m_{plat}=0.5 kg and m_{cart}=0.25 kg.

The paths are of Lissajous type

$$\boldsymbol{p}(u) = \begin{bmatrix}x_P\\y_P\\z_P\end{bmatrix} = \begin{bmatrix}x_0\sin(\omega_x u + \varphi_x)\\y_0\sin(\omega_y u + \varphi_y)\\PQ\end{bmatrix} \tag{18}$$

with $\omega_x = 6\pi$, $\omega_y = 4\pi$, $\varphi_x = \frac{\pi}{2}$, $\varphi_y = 0$ and 0<u<1. Point Q (the extruder nozzle) is supposed to move on the horizontal plane at z=0 at constant speed v along the path. The

path has been discretized with a uniform mesh of points corresponding to the position of the end effector at successive time intervals T_s. The values u_k are estimated iteratively with the following second order Taylor series, in which vector $\boldsymbol{p}$ denotes the position of the end effector. This equation is valid in case speed v is constant [10]:

$$u_{k+1} = u_k + T_s \frac{v}{\left|\frac{d\boldsymbol{p}}{du}\right|_k} - \frac{T_s^2}{2} v^2 \left[\frac{\frac{d\boldsymbol{p}}{du}^T \cdot \frac{d^2\boldsymbol{p}}{du^2}}{\left|\frac{d\boldsymbol{p}}{du}\right|^4} \right]_k \tag{19}$$

Fig. 3 illustrates the architecture of the machine, with also the path on the printing bed.

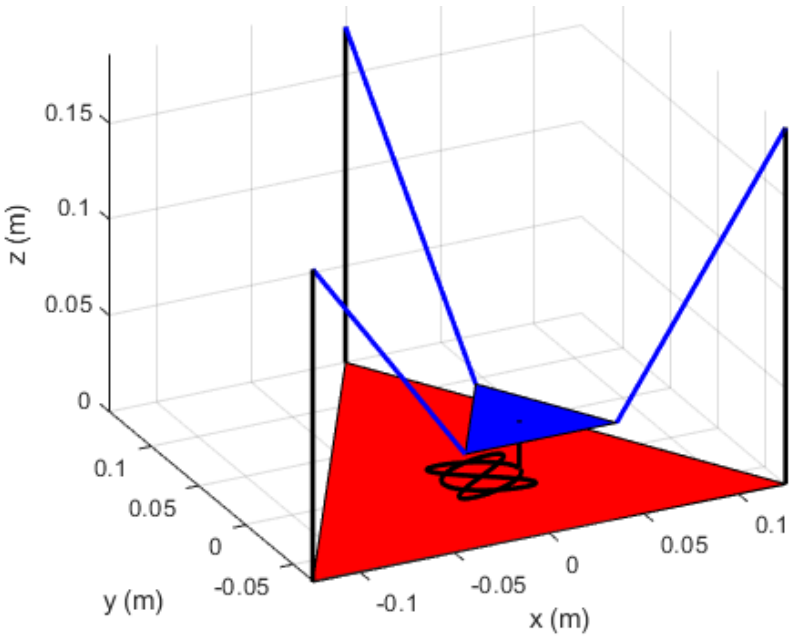

Fig. 3. Architecture of the 3D printer

Fig. 4 on top shows force Q_1 at different printing speeds (10, 50 and 200 mm/s). It is visible the contribution of inertia forces, which become important increasing speed v. It has been verified that the sum of the actuators forces at small speeds coincides with the total gravity force of the suspended masses (about 13.4 N), see fig. 4 at bottom.

In order to further check the results, the time rate of the total energy (potential and kinetic energy) has been compared with the input mechanical power generated by actuators:

$$\frac{d}{dt}(K + U) = Q_1\dot{q}_1 + Q_2\dot{q}_2 + Q_3\dot{q}_3 \tag{20}$$

Fig. 5 compares the two members of Eq. (20), which are found to be coincident, proving the correctness of the results.

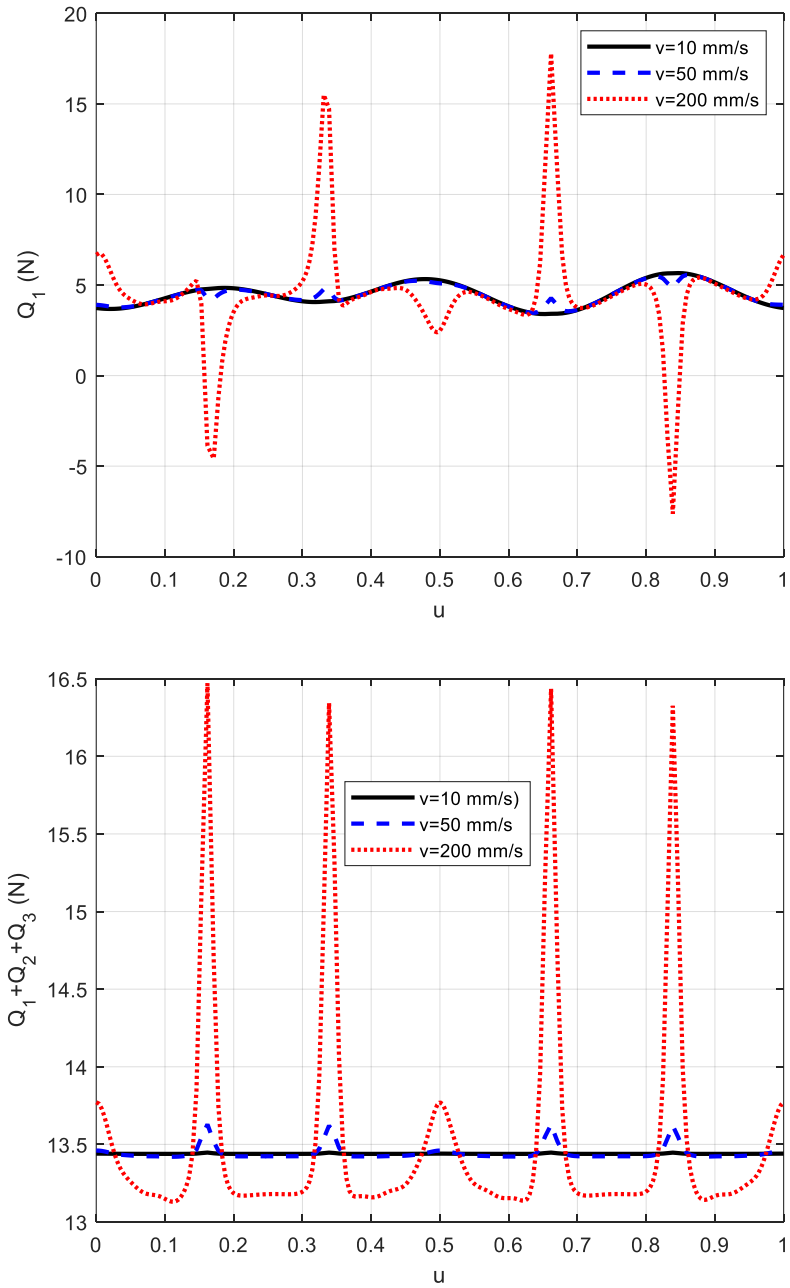

Fig. 4. Actuator force Q_1 (top) and sum of actuators forces (bottom) at different printing speeds *v*.

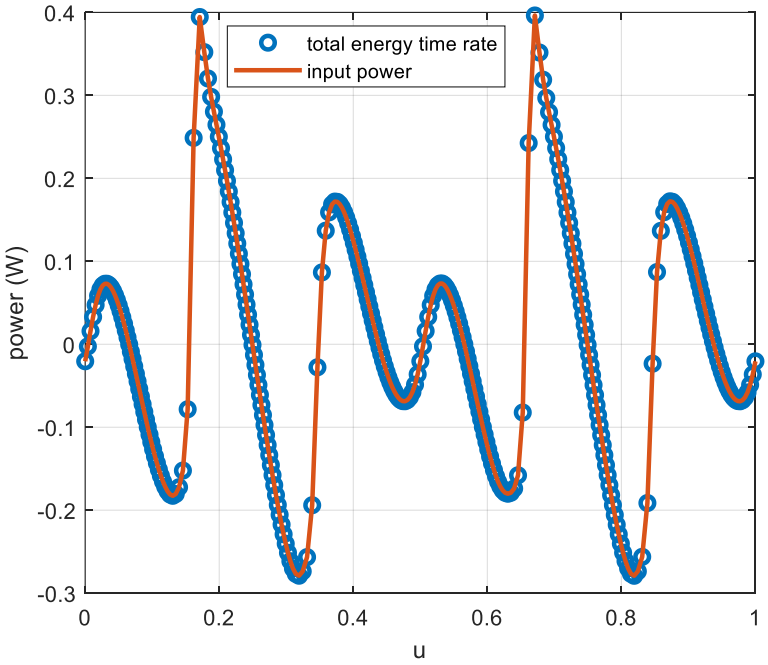

Fig. 5. Comparison of the total energy time rate and the input mechanical power with v=200 mm/s

6 Conclusions

The direct and inverse kinematics of a delta prismatic robot have been detailed in this paper, together with the dynamic study, carried out with the Lagrangian approach with multipliers. The results have been checked with the principle of energy conservation and checking that at small speeds the total actuators forces coincide with the total weight of the suspended masses. The influence of the inertia forces on the actuators forces is visible increasing the printing speed. The study has carried out in absence of friction and other dissipations for a preliminary set up of the model. Future activity could involve the introduction of dissipative actions in order to have a more realistic model.

References

1. Clavel, R.: Delta, a fast robot with parallel geometry. In: Proceedings of the 18th International Symposium on Industrial Robots, 91–100. Lausanne, France, 26–28 April 1988.
2. https://reprap.org/wiki/Rostock
3. https://reprap.org/wiki/Kossel

4. López, M., Castillo, E., García, G., & Bashir, A.: Delta robot: Inverse, direct, and intermediate Jacobians. Proceedings of the Institution of Mechanical Engineers, Part C: Journal of Mechanical Engineering Science, 220(1), 103–109 (2006).
5. Zhao, Y.: Singularity, isotropy, and velocity transmission evaluation of a three translational degrees-of-freedom parallel robot. Robotica, 31(2), 193-202 (2013).
6. http://fab.cba.mit.edu/classes/863.15/section.CBA/people/Spielberg/Rostock_Delta_Kinematics_3.pdf
7. Tsai, L.W.: Robot analysis: the mechanics of serial and parallel manipulators. John Wiley & Sons, NY (1999).
8. Staicu, S. and Carp-Ciocardia D. C.: Dynamic analysis of Clavel's Delta parallel robot. In: 2003 IEEE International Conference on Robotics and Automation, (3), 4116-4121. Taipei, Taiwan, (2003).
9. Brinker, J., Corves, B., Wahle, M.: A Comparative Study of Inverse Dynamics based on Clavel's Delta robot. In: The 14th IFToMM World Congress, 89-98, Taipei (Taiwan) (2015).
10. Biagiotti, L. Melchiorri, C.: Trajectory Planning for Automatic Machines and Robots (2010).